Pergamon

Int. J. Solids Structures Vol. 33, No. 20–22, pp. 3309–3326, 1996

0020–7683/96 $15.00 + .00

0020-7683(95)00262-6

A COMPARISON OF THREE-DIMENSIONAL CONTINUUM AND SHELL ELEMENTS FOR FINITE PLASTICITY

P. WRIGGERS, R. EBERLEIN and S. REESE
Institute for Mechanics, TH Darmstadt, Hochschulstr. 1, 64289 Darmstadt, Germany

Abstract—For three-dimensional continuum elements in solid mechanics crucial developments were achieved by Simo and Armero [*Int. J. Numer. Meth. Engng* **33,** 1413–1449 (1992)] and Simo *et al.* [*Comput. Meth. Appl. Mech. Engng* **110,** 359–386 (1993)] recently. These elements are locking free and show superior bending behaviour even for large strains. Naturally, solid elements are easier to develop and to implement than shell elements. This fact motivates a comparison of continuum and shell elements for thin shell problems. Thus, in this paper, continuum and shell formulations are compared for finite elasto-plastic deformations. Copyright © 1996 Elsevier Science Ltd.

1. INTRODUCTION

Deep drawing processes of metal sheets can be discretized by membrane or shell elements which are able to undergo elasto-plastic deformations. These elements are often highly sophisticated. This is mainly due to two reasons. The first is associated with the fact that finite deformations of shells need a special treatment of the rotational degrees of freedom. Different approaches are possible to formulate finite rotation shell theories, these range from the degenerated solid approach, Ramm (1976), Hughes *et al.* (1981), to different shell models, Schoop (1986), Simo *et al.* (1990), Wriggers and Gruttmann (1993), Basar and Ding (1990) or Wagner and Gruttmann (1994), to name but a few. The second reason is related to the formulation of the constitutive equations which have to be projected onto the shell mid-surface. This process often involves some simplifications or, if these are not acceptable, higher order shell theories taking into account thickness change or even warping deformations in the cross sections. Here two main guidelines can be followed. One is the use of integrated flow rules, formulated in shell resultants forces and moments, see e.g. Simo and Kennedy (1992). The other employs constitutive equations in different layers over the shell thickness and thus needs an integration in thickness direction, see e.g. Parisch (1991), Hughes *et al.* (1981) or Büchter *et al.* (1994).

Due to the latest development of two- and three-dimensional finite elements in solids it is possible to use three-dimensional brick elements for moderately thick and even thin shells. The application of solid elements to shell problems has a long history. Starting with the work of Zienkiewicz *et al.* (1971), many scientists have applied degenerated solid elements for shell problems. However, up to the work of Simo and Armero (1992) and Simo *et al.* (1993) there was no solid element for large strains available, which is locking free and depicts a superior bending behaviour. It is easy to see that an eight-node solid brick incorporates the kinematical relations of a shear-elastic element with thickness change in the normal direction to the shell midsurface. Thus choosing one brick element over the shell thickness yields the desired features of an even enhanced shell model incorporating shear deformations and thickness change. Furthermore, solid elements are a lot easier to develop and to implement, especially since the three-dimensional constitutive equations for inelastic materials can be applied without modifications.

The question now is whether these new classes of solid elements can be applied not only to thick shell but also to thin shell problems, depicting the same efficiency as shell elements. The latter can only be the case when a discretization, with only one solid element over the shell thickness, is sufficient. Then a four-node shell element with 5 or 6 d.f. per

node has to be compared with an eight-node solid brick element with three degrees of freedom per node, which generally leads to the same total number of unknowns. In the case of geometrically linear thin shell problems it has been shown that newly developed stabilized, enhanced solid elements are able to replace shell elements (Korelc and Wriggers, 1995). Thus the enhanced element technology should also work for large deformations and strains.

In this contribution we aim to develop a simple shell element for large strains and rotations, and compare it to three-dimensional elements based on the enhanced strain approach, see Simo *et al.* (1993), when applied to thin shell problems undergoing large inelastic strains. The shell element is based on a quasi-Kirchhoff-theory, which means that the assumption of the classical Kirchhoff–Love kinematic is enforced via a penalty constraint. The constitutive relations for the shell are the same as for the three-dimensional brick element. However, within the thin shell assumptions the constitutive equation is specialized for plane stress, leading to the simplest possible shell model which is valid for thin shells. The thickness change can be computed from additional constraint equations, such as the incompressibility of plastic deformations. Within the solid and shell element we apply constitutive equations for metal plasticity based on von Mises flow rule for finite elasticity and finite plasticity.

The paper is organized as follows. In Section 2, the formulation underlying the simple shell element described above is presented. Then in Section 3 the elasto-plastic relations for finite strains are developed for the three-dimensional theory and then specialized for the shell. In Section 4 two examples are presented which include finite plastic strains and comparisons of three-dimensional and shell solutions. Here the limitations of the different approaches will be discussed. The examples show the performance of shell and continuum elements in cases of different aspect ratios of thickness to mean curvature radius. For this purpose, we first investigate axisymmetrical shells for parameter studies. Then, in a final example of a thin cylindrical shell undergoing finite elasto-plastic deformations, the shell and continuum formulation are compared.

2. SHELL THEORY

The underlying shell theory applied in subsequent numerical examples is based on a so-called "quasi-Kirchhoff-theory" which was derived in detail for axisymmetric shell elements by Eberlein *et al.* (1993). For the current quadrilateral element formulation a Lagrangian description of geometry was chosen. Bilinear shape functions were used within an isoparametric concept. Eventually a five-parameter theory is obtained which accounts for finite plastic deformations of thin shells.

An arbitrary point in shell space is determined by the basic kinematic assumption

$$\mathbf{x}(\xi^1, \xi^2, \xi^3) = \boldsymbol{\phi}(\xi^1, \xi^2) + \xi \mathbf{d}(\xi^1, \xi^2); \quad \xi = \xi^3, \tag{1}$$

where $\boldsymbol{\phi}$ denotes the position vector with respect to the current shell mid-surface and $\mathbf{d}$ the director vector of unit length. $\xi^i|_{i=1,2,3}$ are curvilinear Gaussian co-ordinates. The corresponding base vectors are given subsequently

$$\begin{aligned} \mathbf{g}_\alpha &= \boldsymbol{\phi}_{,\alpha} + \xi \mathbf{d}_{,\alpha} = \mathbf{a}_\alpha + \xi \mathbf{d}_{,\alpha}; \quad \alpha = 1, 2, \\ \mathbf{g}_3 &= \mathbf{d}. \end{aligned} \tag{2}$$

Furthermore we have the constraint equation $\mathbf{d} - \mathbf{n} \stackrel{!}{=} \mathbf{0}$ with $\mathbf{n}$ representing the normal vector to the current shell mid-surface. Therefore $\mathbf{a}_\alpha \cdot \mathbf{d} = 0$ must be fulfilled. For a Lagrangian description the components of the right Cauchy–Green tensor $\mathbf{C}$ have to be provided. The covariant components of $\mathbf{C}$ read

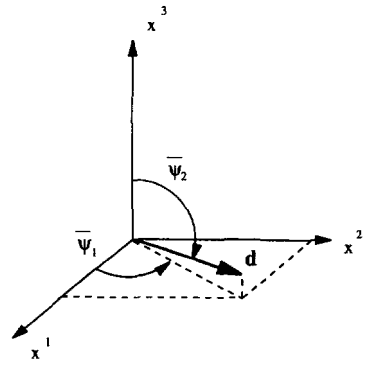

Fig. 1. Rotational description of **d**.

$$C_{ij} = \mathbf{g}_i \cdot \mathbf{g}_j. \tag{3}$$

The referential position vector of the mid-surface $\boldsymbol{\Phi}$ and $\boldsymbol{\phi}$ are connected by a displacement vector **u**

$$\boldsymbol{\phi} = \boldsymbol{\Phi} + \mathbf{u}. \tag{4}$$

For further derivation it is helpful to split **C** into three parts

$$\mathbf{C} = \mathbf{C}^{\mathrm{m}} + \mathbf{C}^{\mathrm{s}} + \xi \mathbf{C}^{\mathrm{b}}, \tag{5}$$

where m, s, b represent membrane, shear and bending terms, respectively. Terms quadratic in ξ are neglected due to the thin shell limit. With (2) the non-zero components of **C** can be written as

$$\begin{aligned} \mathbf{C}^{\mathrm{m}}_{\alpha\beta} &= \mathbf{a}_\alpha \cdot \mathbf{a}_\beta, \\ \mathbf{C}^{\mathrm{s}}_{\alpha 3} &= 2\mathbf{a}_\alpha \cdot \mathbf{d} \stackrel{!}{=} 0, \\ \mathbf{C}^{\mathrm{b}}_{\alpha\beta} &= \mathbf{a}_\alpha \cdot \mathbf{d}_{,\beta} + \mathbf{a}_\beta \cdot \mathbf{d}_{,\alpha}. \end{aligned} \tag{6}$$

The director vector **d** in eqn (6) is formulated in terms of two independent rotation angles $(\bar{\psi}_1, \bar{\psi}_2)$ as shown in Fig. 1. This strategy was applied within a classical shell concept by Wagner and Gruttmann (1994). An additive update of (ψ_1^0, ψ_2^0) with respect to the reference configuration yields the angles $(\bar{\psi}_1, \bar{\psi}_2)$ in the deformed configuration

$$\begin{aligned} \bar{\psi}_1 &= \psi_1^0 + \psi_1, \\ \bar{\psi}_2 &= \psi_2^0 + \psi_2. \end{aligned} \tag{7}$$

Henceforth **d** can be written explicitly as

$$\mathbf{d} = \begin{Bmatrix} \cos\bar{\psi}_1 \sin\bar{\psi}_2 \\ \sin\bar{\psi}_1 \sin\bar{\psi}_2 \\ \cos\bar{\psi}_2 \end{Bmatrix}. \tag{8}$$

From Fig. 1 we can observe that for ψ_2^0 equal to zero, ψ_1^0 is not determined uniquely. In this special case it is necessary to define an associated value of ψ_1^0. Otherwise the rotational description is valid without restrictions.

The finite element formulation can be derived in a straightforward manner now. For our "quasi-Kirchhoff-approach" we impose the transverse shear strains $E^s_{\alpha 3}$ to be zero. This is achieved by adding a penalty term to the weak form of equilibrium:

$$g(\mathbf{v}, \delta\mathbf{v}) = \frac{1}{2}\int_{\beta_0} S_{\alpha\beta}\delta C_{\alpha\beta}\,\mathrm{d}V + \varepsilon \int_{\beta_0} C^s_{\alpha 3}\delta C^s_{\alpha 3}\,\mathrm{d}V - g_a(\mathbf{v}, \delta\mathbf{v}) = 0, \tag{9}$$

where $\mathbf{v} = \{u_1, u_2, u_3, \psi_1, \psi_2\}^{\mathrm{T}}$, ε is a penalty parameter and g_a denotes the virtual work of external loads. The general nonlinearity of eqn (9) in $\mathbf{v}$ demands a consistent linearization of all equations as shown in detail in e.g. Eberlein *et al.* (1993) for axisymmetrical applications. Thus quadratic convergence behaviour is achieved in the solution process. The constitutive equations and linearization for large plastic deformations will be derived in the next section.

3. FINITE PLASTICITY

3.1. *Weak form*

Enhanced strain element formulations have the advantage that they show locking-free behaviour for incompressible problems as well as for bending situations (see Simo and Armero, 1992; Simo *et al.*, 1993 and Wriggers and Hueck, 1995). This is achieved by working with the modified deformation gradient

$$\bar{\mathbf{F}} = \mathbf{F} + \bar{\mathbf{H}} = \mathbf{1} + \underbrace{\operatorname{grad}\mathbf{u}}_{\mathbf{H}} + \bar{\mathbf{H}}, \tag{10}$$

where $\bar{\mathbf{H}}$ represents an additional displacement gradient. Since $\bar{\mathbf{F}} - \mathbf{1} \neq \operatorname{grad}\mathbf{u}$, the development of enhanced strain element formulations is based on the Hu–Washizu variational principle (see Simo and Rifai, 1990). However, in this paper we are dealing with elasto-plastic problems, in which case the local equations cannot be derived from a potential.

We start with the Euler differential equations:

$$\operatorname{div}\mathbf{P} + \rho_0\hat{\mathbf{b}} = \mathbf{0} \quad \text{and} \quad \bar{\mathbf{H}} = \mathbf{0}. \tag{11}$$

Here, $\rho_0\hat{\mathbf{b}}$ represents the body force and $\mathbf{P}$ the first Piola–Kirchhoff stress tensor. Multiplication of these by the test functions $\boldsymbol{\eta}$ and $\boldsymbol{\kappa}$, respectively, followed by integration over the reference configuration β_0, leads to

$$\int_{\beta_0} (\operatorname{div}\mathbf{P} + \rho_0\hat{\mathbf{b}})\cdot\boldsymbol{\eta}\,\mathrm{d}V = 0 \quad \text{and} \quad \int_{\beta_0} \bar{\mathbf{H}} : \boldsymbol{\kappa}\,\mathrm{d}V = 0. \tag{12}$$

Via the divergence theorem, eqn (12) can be transformed into the standard weak form

$$\int_{\beta_0} \mathbf{P} : \operatorname{grad}\boldsymbol{\eta}\,\mathrm{d}V - \underbrace{\int_{\beta_0} \rho_0\hat{\mathbf{b}}\cdot\boldsymbol{\eta}\,\mathrm{d}V - \int_{\partial B_{0P}} \hat{\mathbf{t}}\cdot\boldsymbol{\eta}\,\mathrm{d}A}_{-g_a} = 0, \tag{13}$$

where $\hat{\mathbf{t}}$ denotes the vector of the prescribed surface loads, and $\mathrm{d}A$ an infinitesimal surface element with respect to the reference configuration. Since the modification of the material deformation gradient is not physical, the work due to $\bar{\mathbf{H}}$ should be zero, i.e.

$$\int_{\beta_0} \mathbf{P} : \bar{\mathbf{H}}\,\mathrm{d}V = 0 \tag{14}$$

(see Simo and Armero, 1992). The variation of eqn (14) yields

$$\int_{\beta_0} \delta\mathbf{P}:\bar{\mathbf{H}}\,\mathrm{d}V+\int_{\beta_0}\mathbf{P}:\delta\bar{\mathbf{H}}\,\mathrm{d}V=0\Rightarrow\int_{\beta_0}\bar{\mathbf{H}}:\delta\mathbf{P}\,\mathrm{d}V=-\int_{\beta_0}\mathbf{P}:\delta\bar{\mathbf{H}}\,\mathrm{d}V. \tag{15}$$

If $\delta\mathbf{P}$ is identified with $\boldsymbol{\kappa}$, and the test function $\boldsymbol{\eta}$ is replaced by the virtual displacement vector $\delta\mathbf{u}$, eqn (10) can be written as

$$\begin{aligned}\int_{\beta_0}\hat{\mathbf{P}}(\bar{\mathbf{F}}):\operatorname{grad}\delta\mathbf{u}\,\mathrm{d}V-g_a&=0,\\ \int_{\beta_0}\hat{\mathbf{P}}(\bar{\mathbf{F}}):\delta\bar{\mathbf{H}}\,\mathrm{d}V&=0.\end{aligned} \tag{16}$$

Here, $\mathbf{P}=\hat{\mathbf{P}}(\bar{\mathbf{F}})$ is a function of the modified material deformation gradient $\bar{\mathbf{F}}$, and g_a denotes the virtual work of the external loads. Using the relation $\mathbf{P}=\tau\cdot\bar{\mathbf{F}}^{-\mathrm{T}}$ between $\mathbf{P}$ and the Kirchhoff stress tensor $\tau=\hat{\tau}(\bar{\mathbf{F}})$, we finally obtain

$$\begin{aligned}\hat{g}_b(\mathbf{F},\bar{\mathbf{H}})&=\int_{\beta_0}\hat{\tau}(\bar{\mathbf{F}}):\operatorname{sym}(\operatorname{grad}\delta\mathbf{u}\cdot\bar{\mathbf{F}}^{-1})\,\mathrm{d}V-g_a=0,\\ \hat{g}_g(\mathbf{F},\bar{\mathbf{H}})&=\int_{\beta_0}\hat{\tau}(\bar{\mathbf{F}}):\operatorname{sym}(\delta\bar{\mathbf{H}}\cdot\bar{\mathbf{F}}^{-1})\,\mathrm{d}V=0.\end{aligned} \tag{17}$$

3.2. *Calculation of the Kirchhoff stress tensor*

3.2.1. *Product formula algorithm.* In contrast to purely hyperelastic material behaviour, the stresses are restricted to the domain described by the yield criterion $\Phi\leqslant 0$ in plasticity. An iterative solution procedure for the stresses is then given by the so-called return mapping algorithms. In this work the product formula algorithm proposed by Simo (1992) will be used, which we summarize briefly. However, the treatment of the spectral decomposition will be different.

With the multiplicative decomposition $\bar{\mathbf{F}}=\bar{\mathbf{F}}_{\mathrm{e}}\cdot\bar{\mathbf{F}}_{\mathrm{p}}$ of the modified material deformation gradient into elastic ($\bar{\mathbf{F}}_{\mathrm{e}}$) and plastic ($\bar{\mathbf{F}}_{\mathrm{p}}$) parts, the elastic left Cauchy–Green tensor $\bar{\mathbf{b}}_{\mathrm{e}}$ is calculated by

$$\bar{\mathbf{b}}_{\mathrm{e}}=\bar{\mathbf{F}}_{\mathrm{e}}\cdot\bar{\mathbf{F}}_{\mathrm{e}}^{\mathrm{T}}=\bar{\mathbf{F}}\cdot\bar{\mathbf{C}}_{\mathrm{p}}^{-1}\cdot\bar{\mathbf{F}}^{\mathrm{T}}. \tag{18}$$

Thus, $\bar{\mathbf{b}}_{\mathrm{e}}$ is given by the push-forward transformation of the inverse of the plastic Cauchy–Green tensor $\bar{\mathbf{C}}_{\mathrm{p}}=\bar{\mathbf{F}}_{\mathrm{p}}^{\mathrm{T}}\cdot\bar{\mathbf{F}}_{\mathrm{p}}$. Assuming that the specific free energy $\Psi=\hat{\Psi}(\bar{\mathbf{b}}_{\mathrm{e}},\xi)$ depends only on $\bar{\mathbf{b}}_{\mathrm{e}}$ and the internal strain-like variable ξ, called the equivalent plastic strain, the second law of thermodynamics yields under the restriction of isotropy the constitutive relations

$$\tau=2\rho_0\frac{\partial\Psi}{\partial\bar{\mathbf{b}}_{\mathrm{e}}^{-}}\cdot\bar{\mathbf{b}}_{\mathrm{e}},\quad q=-\frac{\partial\Psi}{\partial\xi} \tag{19}$$

and the dissipation inequality

$$-\tfrac{1}{2}\tau:[(\mathscr{L}_v\bar{\mathbf{b}}_{\mathrm{e}})\cdot\bar{\mathbf{b}}_{\mathrm{e}}^{-1}]-q\dot{\xi}\geqslant 0. \tag{20}$$

$\mathscr{L}_v\bar{\mathbf{b}}_{\mathrm{e}}$ is referred to as the Lie derivative $\mathscr{L}_v\bar{\mathbf{b}}_{\mathrm{e}}=\dot{\bar{\mathbf{b}}}_{\mathrm{e}}-\bar{\mathbf{l}}\cdot\bar{\mathbf{b}}_{\mathrm{e}}-\bar{\mathbf{b}}_{\mathrm{e}}\cdot\bar{\mathbf{l}}^{\mathrm{T}}$. The dot marks a material time derivative and $\bar{\mathbf{l}}=\dot{\bar{\mathbf{F}}}\cdot\bar{\mathbf{F}}^{-1}$ represents the spatial velocity gradient.

The evolution equations for $(\mathscr{L}_v\bar{\mathbf{b}}_{\mathrm{e}})\cdot\bar{\mathbf{b}}_{\mathrm{e}}^{-1}$ and $\dot{\xi}$

$$-\tfrac{1}{2}\mathscr{L}_v\bar{\mathbf{b}}_e = \gamma\left(\frac{\partial\Psi}{\partial\tau}\cdot\bar{\mathbf{b}}^e\right),$$

$$\dot{\xi} = \gamma\left(\frac{\partial\Psi}{\partial q}\right), \tag{21}$$

$$\gamma \geqslant 0, \quad \Psi = \hat{\Psi}(\tau, q) \leqslant 0, \quad \gamma\Psi = 0, \tag{22}$$

can be derived by the postulate of maximum dissipation (see Simo and Miehe, 1992). They represent associative flow rules. γ denotes the slip rate.

The problem of calculating $\bar{\mathbf{b}}_e$, ξ, τ and Φ is solved by an operator split into an elastic predictor and a plastic corrector, see e.g. Simo and Ortiz (1985). To carry out the first operation (calculation of the trial elastic state), Simo (1992) introduced a so-called relative deformation gradient:

$$\mathbf{f} = \frac{\partial\mathbf{x}}{\partial\mathbf{x}_{n-1}} = \frac{\partial\mathbf{x}}{\partial\mathbf{X}}\cdot\frac{\partial\mathbf{X}}{\partial\mathbf{x}_{n-1}} = \mathbf{F}\cdot\mathbf{F}_{n-1}^{-1}. \tag{23}$$

For enhanced strain element formulations we use, instead of $\mathbf{f}$, the modified relative deformation gradient $\bar{\mathbf{f}} = \bar{\mathbf{F}}\cdot\bar{\mathbf{F}}_{n-1}^{-1}$, which coincides for $\bar{\mathbf{H}} = \mathbf{0}$ with eqn (23). $\mathbf{f}$ relates the position vector $\mathbf{x}$ of the current configuration (time t_n) to the position vector $\mathbf{x}_{n-1}$ of the configuration at the time t_{n-1}. The trial elastic state is now given by means of $\bar{\mathbf{f}}$ with

$$\bar{\mathbf{b}}_e^{tr} = \bar{\mathbf{f}}\cdot\bar{\mathbf{b}}_{en-1}\cdot\bar{\mathbf{f}}^T \quad \text{and} \quad \xi = \xi^{tr} = \xi_{n-1}. \tag{24}$$

Physically, this means that the plastic flow is frozen at the state of time t_{n-1}. If the trial elastic state is admissible, i.e. it does not violate the inequality $\Phi \leqslant 0$, we have

$$\tau^{tr} = 2\rho_0\left.\frac{\partial\Psi}{\partial\bar{\mathbf{b}}_e}\right|_{\bar{\mathbf{b}}_e=\bar{\mathbf{b}}_e^{tr}}\cdot\bar{\mathbf{b}}_e^{tr} \quad \text{and} \quad q^{tr} = -\left.\frac{\partial\Psi}{\partial\xi}\right|_{\xi=\xi^{tr}}. \tag{25}$$

Otherwise, the return mapping algorithm is applied to fulfill $\Phi = 0$. Since during this phase the position $\mathbf{x} = \mathbf{x}^{tr}$ is held fixed, we obtain (with then $\bar{\mathbf{l}} = \mathbf{0}$) the first order differential equation

$$\dot{\bar{\mathbf{b}}}_e = \mathscr{L}_v\bar{\mathbf{b}}_e = -2\gamma\frac{\partial\Phi}{\partial\tau}\cdot\bar{\mathbf{b}}_e, \tag{26}$$

from which follows the product formula

$$\tilde{\bar{\mathbf{b}}}_e = \exp\left[-2\underbrace{(t-t_n)\gamma}_{\Delta\gamma}\frac{\partial\Phi}{\partial\tau}\right]\cdot\bar{\mathbf{b}}_{en} \quad \text{with} \quad \bar{\mathbf{b}}_{en} = \bar{\mathbf{b}}_e|_{t=t_n} = \bar{\mathbf{b}}_e^{tr}. \tag{27}$$

Note that $\Delta\gamma(\partial\Phi/\partial\tau]$ is considered to be constant during the time interval $[t_n, t)$, and that $\tilde{\bar{\mathbf{b}}}_e$ commutes with τ due to the assumption of isotropy. Furthermore, $\bar{\mathbf{b}}_e^{tr}$ and its principal axes are held fixed during the return mapping, so that with the spectral decompositions

$$\tilde{\bar{\mathbf{b}}}_e = \sum_{A=1}^{3}\lambda_{Ae}^2\mathbf{n}_A^{tr}\otimes\mathbf{n}_A^{tr}, \quad \bar{\mathbf{b}}_e^{tr} = \sum_{A=1}^{3}\lambda_{Ae}^{tr2}\mathbf{n}_A^{tr}\otimes\mathbf{n}_A^{tr}, \quad \tau = \sum_{A=1}^{3}\tau_A\mathbf{n}_{Ae}^{tr}\otimes\mathbf{n}_A^{tr}. \tag{28}$$

Equation (27) can be written in principal value form as

$$\lambda_{Ae}^2 = \exp\left[-2\Delta\gamma\frac{\partial\Phi}{\partial\tau_A}\right]\lambda_{Ae}^{tr2} \tag{29}$$

($A = 1, 2, 3$). Taking the logarithm of eqn (29) finally yields

$$\varepsilon_{Ae}^{tr} = \varepsilon_{Ae} + \Delta\gamma\frac{\partial\Phi}{\partial\tau_A}, \tag{30}$$

where ε_{Ae} represent the logarithmic principal stretches $\ln\lambda_{Ae}$. Here, the main advantage of the product formula algorithm becomes clear: by using logarithmic strain measures, an *additive* split of the trial elastic strain into elastic and plastic parts is obtained (see Simo, 1992 for a more detailed derivation). The equivalent plastic strain ξ is calculated by the approximation

$$\tilde{\xi} = \xi_n + \Delta\gamma\frac{\partial\Phi}{\partial q}. \tag{31}$$

To solve the non-linear equations

$$\begin{aligned} r_A &= \hat{r}_A(\varepsilon_{Ae}, \Delta\gamma, \tau_A) = \varepsilon_{Ae}^{tr} - \varepsilon_{Ae} - \Delta\gamma\frac{\partial\Phi}{\partial\tau_A} = 0 \\ \Phi &= \hat{\Phi}(\tau_A, q) \qquad\qquad = 0, \end{aligned} \tag{32}$$

Newton's method is applied. The principal Kirchhoff stresses are then calculated by

$$\tau_A = 2\rho_0\lambda_{Ae}\frac{\partial\Psi}{\partial\lambda_{Ae}} = 2\rho_0\frac{\partial\Psi}{\partial\varepsilon_{Ae}}, \tag{33}$$

where the specific free energy $\Psi = \bar{\Psi}(\varepsilon_{Ae}, \xi)$ is now written as a function of the logarithmic elastic principal stretches and the equivalent plastic strain ξ. In particular, for the special case of a Von Mises yield criterion with linear isotropic hardening:

$$\Phi_{\text{Mises}} = \|\operatorname{dev}\tau\| - \sqrt{\tfrac{2}{3}}(\tau_Y - q), \quad q = -H\xi \tag{34}$$

(τ_Y yield stress, H hardening parameter), and a quadratic strain energy function

$$W = \rho_0\Psi = \mu(\varepsilon_{1e}^2 + \varepsilon_{2e}^2 + \varepsilon_{3e}^2) + \frac{\Lambda}{2}(\varepsilon_{1e} + \varepsilon_{2e} + \varepsilon_{3e})^2 + \tfrac{1}{2}H\xi^2, \tag{35}$$

for a closed form solution for Δ_γ can be obtained. If another strain energy function, e.g. the Neo-Hookian, is used, the system (32) has to be solved iteratively.

3.2.2. *Transformation to general coordinate axes.* By the solution of the non-linear eqn (32), the principal values ε_{Ae} and τ_A are determined. However, for the next time step and the solution of the weak form eqn (17), the coefficients of $\bar{\mathbf{b}}_e$ and $\boldsymbol{\tau}$ with respect to general coordinate axes are needed. At this point, we proceed differently from Simo (1992), who used for the representation of $\mathbf{n}_A^{tr} \otimes \mathbf{n}_A^{tr}$ in terms of $\mathbf{b}_e$ the closed-form formula derived by Morman (1986) (see also Simo and Taylor, 1991). In contrast to this, the eigenvectors are determined here explicitly by solving the eigenvalue problem

$$(\bar{\mathbf{b}}_e^{tr} - \lambda_{Ae}^{tr2}\mathbf{1})\mathbf{n}_A^{tr} = 0. \tag{36}$$

With the Cartesian unit vectors $\mathbf{e}_B$ we have the relation

$$\mathbf{n}_A^{\mathrm{tr}} = \sum_{B=1}^{3} (\mathbf{e}_B \otimes \mathbf{e}_B) \cdot \mathbf{n}_A^{\mathrm{tr}} = \sum_{B=1}^{3} \underbrace{(\mathbf{e}_B \cdot \mathbf{n}_A^{\mathrm{tr}})}_{D_{BA}} \mathbf{e}_B = \sum_{B=1}^{3} D_{BA}\mathbf{e}_B \Rightarrow \mathbf{n}_A^{\mathrm{tr}} = D_{bA}\mathbf{e}_b, \tag{37}$$

where the Einstein summation convention holds for lower case Roman and Greek letters. With the principal values of $\bar{\mathbf{b}}_{\mathrm{e}}$ $(i,j = 1,2,3)$

$$b_{i\mathrm{e}}^{\mathrm{prin}} = \exp[2\varepsilon_{i\mathrm{e}}], \quad b_{ij\mathrm{e}}^{\mathrm{prin}} = 0 \quad \text{for} \quad i \neq j, \tag{38}$$

we obtain

$$\bar{\mathbf{b}}_{\mathrm{e}} = b_{ij\mathrm{e}}^{\mathrm{prin}} \mathbf{n}_i^{\mathrm{tr}} \otimes \mathbf{n}_j^{\mathrm{tr}} = \underbrace{D_{ki} b_{ij\mathrm{e}}^{\mathrm{prin}} D_{lj}}_{b_{kl\mathrm{e}}} \mathbf{e}_k \otimes \mathbf{e}_l = b_{kl\mathrm{e}} \mathbf{e}_k \otimes \mathbf{e}_l. \tag{39}$$

The coefficients τ_{ij} are determined analogously. For numerical calculations, it is convenient to take advantage of the symmetry of $\bar{\mathbf{b}}_{\mathrm{e}}$ and $\boldsymbol{\tau}$. Thus vector notation is used, which leads to

$$\hat{\mathbf{b}}_{\alpha\mathrm{e}} = A_{\alpha\beta} \hat{\mathbf{b}}_{\beta\mathrm{e}}^{\mathrm{prin}}, \quad \hat{\boldsymbol{\tau}}_{\alpha} = A_{\alpha\beta} \hat{\boldsymbol{\tau}}_{\beta}^{\mathrm{prin}}, \tag{40}$$

with $\alpha, \beta = 1,2,\ldots,6$. The vectors $\hat{\mathbf{b}}_{\alpha\mathrm{e}}$ and $\hat{\boldsymbol{\tau}}_{\alpha\mathrm{e}}$ are given by

$$\begin{aligned} \{\hat{b}_{\alpha\mathrm{e}}\}^{\mathrm{T}} &= \{b_{11\mathrm{e}}, b_{22\mathrm{e}}, b_{33\mathrm{e}}, b_{12\mathrm{e}}, b_{23\mathrm{e}}, b_{31\mathrm{e}}\}, \\ \{\hat{\tau}_{\alpha\mathrm{e}}\}^{\mathrm{T}} &= \{\tau_{11\mathrm{e}}, \tau_{22\mathrm{e}}, \tau_{33\mathrm{e}}, \tau_{12\mathrm{e}}, \tau_{23\mathrm{e}}, \tau_{31\mathrm{e}}\}, \end{aligned} \tag{41}$$

respectively. The explicit form of the 6×6 transformation matrix $A_{\alpha\beta}$ can be found in Reese (1994) and Reese and Wriggers (1995).

3.3. *Solution of the weak form*

For the solution of the non-linear eqn (17) Newton's method is applied, thus a consistent linearization of eqn (17) is necessary. The Taylor expansion of $\hat{g}_b(\mathbf{F}, \bar{\mathbf{H}}) = 0$ and $\hat{g}_g(\mathbf{F}, \bar{\mathbf{H}}) = 0$ yields

$$\begin{aligned} \hat{g}_b(\mathbf{F}, \bar{\mathbf{H}}) &= \hat{g}_b(\mathbf{F}_0, \bar{\mathbf{H}}_0) + \underbrace{D\hat{g}_b(\mathbf{F}_0, \bar{\mathbf{H}}_0) : \Delta\mathbf{F} + D\hat{g}_b(\mathbf{F}, \bar{\mathbf{H}}) : \Delta\mathbf{H}}_{\Delta\hat{g}_b(\mathbf{F}, \bar{\mathbf{H}})} + |\ldots = 0, \\ \hat{g}_g(\mathbf{F}, \bar{\mathbf{H}}) &= \hat{g}_g(\mathbf{F}_0, \bar{\mathbf{H}}_0) + \underbrace{D\hat{g}_g(\mathbf{F}_0, \bar{\mathbf{H}}) : \Delta\mathbf{F} + D\hat{g}_g(\mathbf{F}, \bar{\mathbf{H}}_0) : \Delta\mathbf{H}}_{\Delta\hat{g}_g(\mathbf{F}, \bar{\mathbf{H}})} + |\ldots = 0, \end{aligned} \tag{42}$$

where e.g.

$$D\hat{g}_b(\mathbf{F}_0, \bar{\mathbf{H}}) : \Delta\mathbf{F} = D\hat{g}_b(\mathbf{F}_0, \bar{\mathbf{H}}) : \mathrm{grad}\, \Delta\mathbf{u} = \frac{\mathrm{d}}{\mathrm{d}\alpha} \hat{g}_b(\mathbf{F}_0 + \alpha\, \Delta\mathbf{F}, \bar{\mathbf{H}})|_{\alpha=0} \tag{43}$$

defines the directional derivative (Gateaux-derivative) of g_b with respect to $\mathbf{F}$. Pulling eqn (17) back to the reference configuration, carrying out the linearization and finally pushing the linearized equation forward to the current configuration leads to

$$\begin{aligned} \Delta\hat{g}_b(\mathbf{F}, \bar{\mathbf{H}}) = \int_{\beta_0} [&(\bar{\mathbf{F}} \cdot \Delta\mathbf{S} \cdot \bar{\mathbf{F}}^{\mathrm{T}}) : \mathrm{sym}(\mathrm{grad}\, \delta\mathbf{u} \cdot \bar{\mathbf{F}}^{-1}) \\ &+ \boldsymbol{\tau} : \mathrm{sym}(\bar{\mathbf{F}}^{-\mathrm{T}} \cdot \Delta\bar{\mathbf{F}}^{\mathrm{T}} \cdot \mathrm{grad}\, \delta\mathbf{u} \cdot \bar{\mathbf{F}}^{-1})]\, \mathrm{d}V + \Delta g_{\alpha}, \end{aligned}$$

$$\Delta\hat{g}_g(\mathbf{F},\bar{\mathbf{H}}) = \int_{\beta_0} [(\bar{\mathbf{F}}\cdot\Delta\mathbf{S}\cdot\bar{\mathbf{F}}^{\mathrm{T}}) : \mathrm{sym}(\delta\bar{\mathbf{H}}\cdot\bar{\mathbf{F}}^{-1}) + \tau : \mathrm{sym}(\bar{\mathbf{F}}^{-\mathrm{T}}\cdot\Delta\bar{\mathbf{F}}^{\mathrm{T}}\cdot\delta\mathbf{H}\cdot\bar{\mathbf{F}}^{-1})]\,\mathrm{d}V, \tag{44}$$

where $\mathbf{S}$ is the second Piola–Kirchhoff stress tensor. The terms Δg_a results from the linearization of the virtual work done by deformation dependent loads (see for more details Sewell, 1966; Schweizerhof and Ramm, 1984; and Simo *et al.*, 1991). Note that the linearization for elasto-plastic problems differs from that for hyperelastic problems only in the calculation of the stress increment $\bar{\mathbf{F}}\cdot\Delta\mathbf{S}\cdot\bar{\mathbf{F}}^{\mathrm{T}}$. Using

$$\mathbf{S} = \bar{\mathbf{F}}^{-1}\cdot\tau\cdot\bar{\mathbf{F}}^{-\mathrm{T}} = \bar{\mathbf{F}}_{pn-1}^{-1}\cdot\underbrace{\bar{\mathbf{F}}_{\mathrm{e}}^{\mathrm{tr}-1}\cdot\tau\cdot\bar{\mathbf{F}}_{\mathrm{e}}^{\mathrm{tr}-\mathrm{T}}}_{\tilde{\mathbf{S}}}\cdot\bar{\mathbf{F}}_{pn-1}^{-\mathrm{T}}, \tag{45}$$

a symmetric stress tensor $\tilde{\mathbf{S}}$ with respect to the fixed plastic intermediate configuration is defined.

We start from the spectral decomposition

$$\tilde{\mathbf{S}} = \sum_{A=1}^{3} \underbrace{\frac{\tau_A}{\lambda_{Ae}^{\mathrm{tr}2}}}_{\tilde{S}_A} \mathbf{N}_{Ap}\otimes\mathbf{N}_{Ap}. \tag{46}$$

The linearization of $\tilde{\mathbf{S}}$ yields

$$\Delta\tilde{\mathbf{S}} = \frac{\partial\tilde{\mathbf{S}}}{\partial\tilde{\mathbf{C}}} : \Delta\tilde{\mathbf{C}} = \sum_{B=1}^{3} \frac{\partial\tilde{\mathbf{S}}}{\partial\varepsilon_{Be}^{\mathrm{tr}}} \frac{\partial\varepsilon_{Be}^{\mathrm{tr}}}{\partial\tilde{\mathbf{C}}} : \Delta\tilde{\mathbf{C}}, \tag{47}$$

with the elastic right Cauchy–Green tensor $\tilde{\mathbf{C}} = \bar{\mathbf{F}}_{\mathrm{e}}^{\mathrm{tr}\mathrm{T}}\cdot\bar{\mathbf{F}}_{\mathrm{e}}^{\mathrm{tr}}$. For the calculation of the partial derivative

$$\frac{\partial\tilde{S}_A}{\partial\varepsilon_{Be}^{\mathrm{tr}}} = \frac{1}{\lambda_{Ae}^{\mathrm{tr}4}}\left(\underbrace{\frac{\partial\tau_A}{\partial\varepsilon_{Be}^{\mathrm{tr}}}}_{C_{AB}^{\mathrm{alg}}}\lambda_{Ae}^{\mathrm{tr}2} - \tau_A 2\lambda_{Ae}^{\mathrm{tr}}\underbrace{\frac{\partial\lambda_{Ae}^{\mathrm{tr}}}{\partial\varepsilon_{Be}^{\mathrm{tr}}}}_{\lambda_{Ae}^{\mathrm{tr}}\delta_{AB}}\right), \tag{48}$$

the algorithmic modulus C_{AB}^{alg} has to be determined, which follows from the linearization of eqn (32) (see e.g. Simo, 1992). Furthermore, the relation

$$2\frac{\partial\varepsilon_{Be}^{\mathrm{tr}}}{\partial\tilde{\mathbf{C}}} = \frac{1}{\lambda_{Be}^{\mathrm{tr}2}}\mathbf{N}_{B\mathrm{p}}\otimes\mathbf{N}_{B\mathrm{p}}, \tag{49}$$

given e.g. by Simo (1992) is used in eqn (47), which yields together with eqn (48)

$$\Delta\tilde{\mathbf{S}} = \left(\sum_{A=1}^{3}\sum_{B=1}^{3}\frac{1}{\lambda_{Ae}^{\mathrm{tr}2}\lambda_{Be}^{\mathrm{tr}2}}(C_{AB}^{\mathrm{alg}} - \tau_A 2\delta_{AB})\mathbf{N}_{A\mathrm{p}}\otimes\mathbf{N}_{A\mathrm{p}}\otimes\mathbf{N}_{B\mathrm{p}}\otimes\mathbf{N}_{B\mathrm{p}}\right) : \lambda_{Be}^{\mathrm{tr}}\Delta\lambda_{Be}^{\mathrm{tr}}\mathbf{N}_{B\mathrm{p}}\otimes\mathbf{N}_{B\mathrm{p}} + \sum_{A=1}^{3}\tilde{S}_A\Delta(\mathbf{N}_{A\mathrm{p}}\otimes\mathbf{N}_{A\mathrm{p}}). \tag{50}$$

On the basis of results in Ogden (1984, pp. 128, 336) the stress and strain increments

$$\Delta\tilde{\mathbf{S}} = \sum_{A=1}^{3} \Delta\tilde{S}_A \mathbf{N}_{Ap} \otimes \mathbf{N}_{Ap} + \sum_{A=1}^{3} \sum_{B\neq A=1}^{3} (\tilde{S}_B - \tilde{S}_A)\Omega_{BA} \mathbf{N}_{Ap} \otimes \mathbf{N}_{Bp},$$

$$\tfrac{1}{2}\Delta\tilde{\mathbf{C}} = \frac{1}{2}\left(\sum_{A=1}^{3} 2\lambda_{Ae}^{tr}\, \Delta\lambda_{Ae}^{tr} \mathbf{N}_{Ap} \otimes \mathbf{N}_{Ap} + \sum_{A=1}^{3} \sum_{B\neq A=1}^{3} (\lambda_{Be}^{tr2} - \lambda_{Ae}^{tr2})\Omega_{BA} \mathbf{N}_{Ap} \otimes \mathbf{N}_{Bp} \right), \tag{51}$$

with

$$\Delta\mathbf{N}_{Bp} = \sum_{C=1}^{3} \underbrace{(\mathbf{N}_{Cp} \cdot \Delta\mathbf{N}_{Bp})}_{\Omega_{CB}} \mathbf{N}_{Cp}, \tag{52}$$

can be calculated. This leads to the incremental constitutive relation

$$\Delta\tilde{\mathbf{S}} = \mathscr{L} : \tfrac{1}{2}\Delta\tilde{\mathbf{C}}, \tag{53}$$

where

$$\begin{aligned} \mathscr{L} &= \sum_{A=1}^{3} \sum_{B=1}^{3} \left(\frac{1}{\lambda_{Ae}^{tr2}\lambda_{Be}^{tr2}} (C_{AB}^{alg} - \tau_A 2\delta_{AB}) \mathbf{N}_{Ap} \otimes \mathbf{N}_{Ap} \otimes \mathbf{N}_{Bp} \otimes \mathbf{N}_{Bp} \right) \\ &\quad + \tfrac{1}{2} \sum_{A=1}^{3} \sum_{B=1}^{3} 2 \frac{\tilde{S}_B - \tilde{S}_A}{\lambda_{Be}^{tr2} - \lambda_{Ae}^{tr2}} (\mathbf{N}_{Ap} \otimes \mathbf{N}_{Bp} \otimes \mathbf{N}_{Ap} \otimes \mathbf{N}_{Bp} + \mathbf{N}_{Ap} \otimes \mathbf{N}_{Bp} \otimes \mathbf{N}_{Bp} \otimes \mathbf{N}_{Ap}) \\ &= L_{abcd}^{prin} \mathbf{N}_{ap} \otimes \mathbf{N}_{bp} \otimes \mathbf{N}_{cp} \otimes \mathbf{N}_{dp} \end{aligned} \tag{54}$$

is the fourth-order constitutive tensor related to the intermediate configuration. Using

$$\bar{\mathbf{F}} \cdot \Delta\mathbf{S} \cdot \bar{\mathbf{F}}^{T} = \bar{\mathbf{F}}_e^{tr} \cdot \Delta\tilde{\mathbf{S}} \cdot \bar{\mathbf{F}}_e^{trT} \quad \text{and} \quad \bar{\mathbf{F}}^{-T} \cdot \Delta\bar{\mathbf{C}} \cdot \bar{\mathbf{F}}^{-1} = \bar{\mathbf{F}}_e^{tr-T} \cdot \Delta\hat{\mathbf{C}} \cdot \bar{\mathbf{F}}_e^{tr-1}, \tag{55}$$

with $\bar{\mathbf{C}} = \bar{\mathbf{F}}^{T} \cdot \bar{\mathbf{F}}$, the constitutive tensor of the current configuration with respect to the principal axes takes the form

$$\mathscr{C} = \underbrace{L_{abcd}^{prin} \lambda_{ae}^{tr} \lambda_{be}^{tr} \lambda_{ce}^{tr} \lambda_{de}^{tr}}_{C_{abcd}^{prin}} \mathbf{n}_a^{tr} \otimes \mathbf{n}_b^{tr} \otimes \mathbf{n}_c^{tr} \otimes \mathbf{n}_d^{tr}. \tag{56}$$

In matrix notation, the coefficients C_{abcd}^{prin} are transformed with respect to general coordinates (see Reese, 1994; Reese and Wriggers, 1995) with

$$\hat{\mathbf{C}}_{\alpha\beta} = A_{\alpha\gamma} \hat{\mathbf{C}}_{\gamma\delta}^{prin} A_{\beta\delta}. \tag{57}$$

3.4. *Application to shells*

The elasto-plastic model for the shells has to be formulated in terms of the reference coordinates, since the current configuration is not easily accessible due to the convected description of the shell surfaces. This approach has been used for membranes by Ibrahimbegović (1994) and will be extended to the quasi-Kirchhoff shell formulation here. Another view was taken in Wriggers *et al.* (1995) who developed under the assumption of small elastic strains a model for finite plastic strains for axisymmetrical shell elements using logarithmic strains.

We make use of eqn (18) which is the "pull back" of $\mathbf{b}_e$ to the reference configuration

$$\mathbf{C}_p^{-1} = \mathbf{F}^{-1} \mathbf{b}_e \mathbf{F}^{-T}. \tag{58}$$

In the algorithmic treatment we need the eigenvalues of $\mathbf{b}_e^{tr}$, which are computed from

$$(\mathbf{b}_e^{tr} - \lambda_{Ae}^{tr2}\,\mathbf{1})\mathbf{n}_A^{tr} = \mathbf{0}. \tag{59}$$

The "pull back" of this eigenvalue problem by $\mathbf{F}_n$ leads to the associated eigenvalue problem in the reference configuration

$$(\mathbf{C}_{pn-1}^{-1} - \lambda_{Ae}^{tr2}\,\mathbf{C}_n^{-1})\mathbf{n}_A^{tr} = \mathbf{0}, \tag{60}$$

where $\mathbf{C}_{pn-1}^{-1}$ describes the known plastic deformation at time t_{n-1}. $\mathbf{C}_n^{-1}$ is computed from eqn (6) as

$$[C_{\alpha\beta}]_n^{-1} = [C_{\alpha\beta}^m + \xi C_{\alpha\beta}^b]^{-1}, \tag{61}$$

for each integration point ξ_p in shell thickness direction. Once $\lambda_{Ae}^{tr^2}$ is computed from eqn (60), eqn (29) can be applied to compute the eigenvalues λ_{Ae}^2 of $\mathbf{b}_e$, and the principal Kirchhoff stresses follow from eqn (33) via a function evaluation with eqn (35) where the logarithmic stretches $\varepsilon_{\alpha e} = \ln \lambda_{\alpha e}$ are used and the plane stress constraint $\tau_3 = 0$ is imposed. Once $\mathbf{b}_{en}$ is known from the solution of eqn (32), the new plastic deformation at time t_n is given by

$$\mathbf{C}_{pn}^{-1} = \mathbf{F}_n^{-1}\mathbf{b}_{en}\mathbf{F}_n^{-T}. \tag{62}$$

Furthermore, the second Piola–Kirchhoff stresses $S^{\alpha\beta}$ needed in the weak form of eqn (9) can be computed from eqn (33) via its principal values

$$S_A = \lambda_{Ae}^{-2}\,\tau_A = 2\rho_0 \frac{\partial \Psi}{\partial \varepsilon_{Ae}} \lambda_{Ae}^{-2}; \quad A = 1, 2. \tag{63}$$

The transformation of S_A to the general coordinate axes and its linearization can then be derived according to the formulation in Section 2 by restricting it to two coordinate directions only.

4. EXAMPLES

4.1. *General remarks*

For the purpose of a comparison between the Kirchhoff shell element formulation and the three-dimensional enhanced strain element formulation two examples have been thoroughly investigated. In both examples we use the strain energy function (35) which is quadratic in the logarithmic strain measure as well as in the equivalent plastic strain. To obtain locking-free behaviour in bending dominated problems a strain profile which is at least linear must be representable inside every element.

Using three-dimensional isoparametric elements this is achieved by the following steps (see for more details Simo *et al.*, 1993). First the material deformation gradient, which is calculated from the standard shape functions $N_I = N_I(\xi, \eta, \chi) = \frac{1}{8}(1+\xi\xi_I)(1+\eta\eta_I)(1+\chi\chi_I)$, $I = 1, 2, \ldots, 8$ (ξ, η and χ are local coordinates), is enhanced by an additional displacement gradient to guarantee the linear completeness of the strain field. Here nine additional degrees of freedom are introduced. Furthermore, for three-dimensional element formulations additional bilinear terms are needed in the strain field. They are provided by another additional displacement gradient which contains three further artificial degrees of freedom. Finally, to obtain locking-free behaviour for distorted element configurations, Simo *et al.* (1993) carried out the calculation of the gradient of the shape functions in the middle point of the elements. Since for the eight-point Gauss quadrature the enhanced strain elements exhibit numerical instabilities, a nine-point Gauss integration (one additional point in the middle of the element) has to be used.

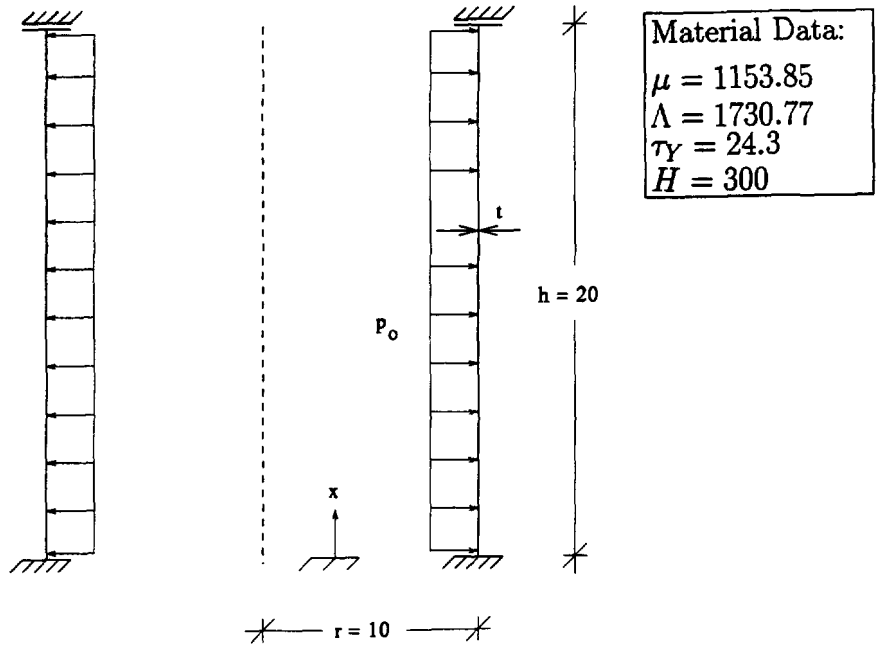

Fig. 2. Initial geometry of the cylinder.

For the "quasi-Kirchhoff-approach" an axisymmetrical as well as a quadrilateral shell element was developed. Standard linear shape functions were used for the axisymmetric conical two-node element and bilinear shape functions $N_I(\xi,\eta) = \frac{1}{4}(1+\xi\xi_I)(1+\eta\eta_I)$; $I = 1$, 2, 3 and 4 for the isoparametric four-node element. A reduced Gauss integration for the penalty term in eqn (9) was applied in both cases.

4.2. *Parameter study for a cylinder under pressure load*

This study shows a comparison of the above-mentioned finite element formulations for various thicknesses t of a cylinder. For this purpose we consider the stresses obtained by:

- axisymmetrical shell elements;
- three-dimensional solid elements;

for the problem as shown in Fig. 2. The cylinder is subjected to a constant pressure load p_0. We chose sufficiently fine meshes for both element types.

In the case of three-dimensional solid elements only a segment of 1° was discretized, this means all brick elements were located along the length of the cylinder which includes just one element layer in thickness direction. A two point Gauss integration was used in thickness direction for the shell elements whereas an eight point rule was applied in the three-dimensional case. So for one element layer in thickness direction, as in the current example, this also means two integration points at the same thickness coordinates for the solid elements as for the shell elements.

In Figs 3 and 4 the axial Kirchhoff stresses τ_x calculated at these Gaussian points are depicted for both element types. Since the lower end of the cylinder is clamped we obtain bending influences in the stresses. Figure 3 shows the stresses at $x = 0.02$ for a thickness range from $t = 2$ to $t = 10^{-4}$. Three facts can be observed from this plot:

(1) For moderately thick and thick shells ($r/t < 5 \times 10^1$) the solutions of both element types differ more and more with increasing thickness. This is due to the fact that no transverse shear deformations were taken into consideration for the shell elements. Therefore the shell solution becomes too stiff (see also Fig. 4).

(2) For $5 \times 10^1 \leqslant r/t \leqslant 10^4$ closely related results are obtained for both element types.

(3) For very thin shells ($r/t > 10^4$) the shell solution converges to the membrane solution $(\tau_x/p_0)(t/r) = 0.3$. The shell elements reach this threshold at $t = 10^{-4}$ without

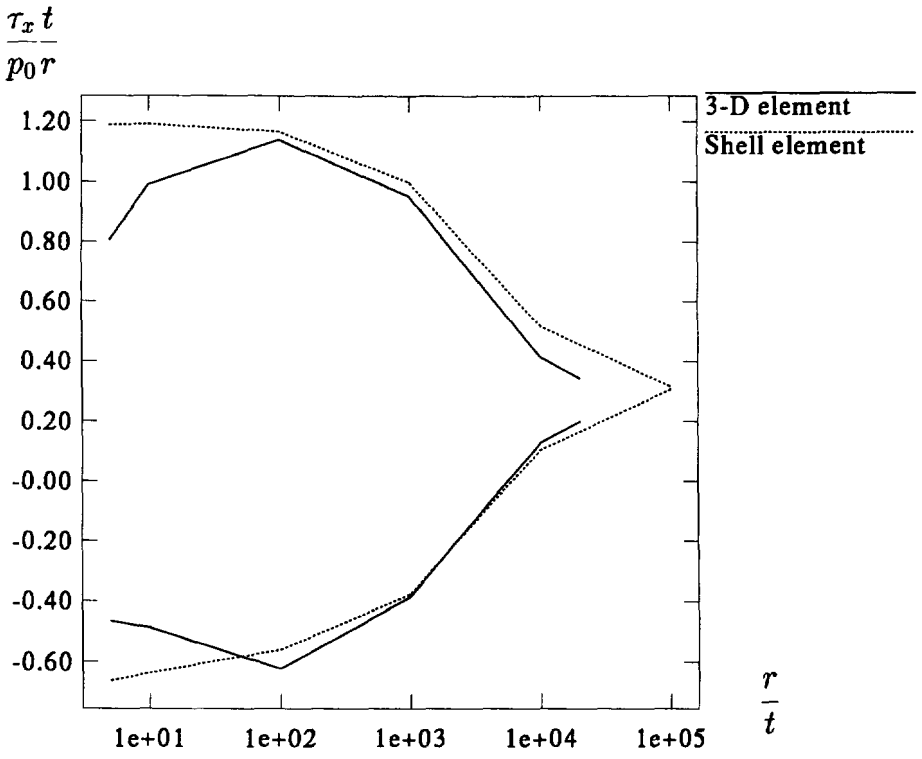

Fig. 3. Stress study for various thicknesses.

numerical problems. The brick elements show numerical ill-conditioning due to severe mesh distortion and the membrane solution cannot be obtained. Yet convergence occurs down to $t = 5 \times 10^{-4}$ which means a remarkable ratio of element height over element thickness of 200.

Figure 4 depicts the Kirchhoff stresses τ_x along the length of the cylinder. Very good correspondence of both solutions can be perceived for $r/t = 100$ and $r/t = 1000$. All stress plots were performed when the cylinder just plastified.

4.3. *Pinched cylinder*

As the second example, the elasto-plastic deformation of a cylinder exposed to two radial pinching displacements in the middle of the structure is considered. Due to the symmetry of the system only an octant of the cylinder is discretized (see Fig. 5). On the boundary $Z = 300$ all nodes are held in X- and Y-directions but can move in the Z-direction. The other boundaries ($X = 0, Y = 0, Z = 0$) represent symmetry planes and are fixed according to the symmetry conditions. This is a classical test example for linear shell elements and has also been considered in Simo and Kennedy (1992). The material parameters are given in Fig. 5, for the plastic material response linear isotropic hardening is assumed.

In the three-dimensional calculation only one element over the thickness has been used. The described shell element is applied with two Gauss points in thickness direction. In Fig. 6 the load–displacements curves for different discretizations are plotted.

Up to a prescribed displacement $v = 180$ (reaction force F) the results of the shell calculation (16×16 and 32×32 elements) agree well with the results of the three-dimensional calculation (32×32 and 40×40 elements). The three-dimensional calculation with 16×16 elements yields results which are too stiff, i.e. the three-dimensional solutions converge more slowly than the shell solution. For $v > 180$, interestingly, the shell curve (16×16) shows periodic load decreases which can be explained by snap-through mechanisms. These are caused by the fact that the plastic zone cannot develop continuously, an

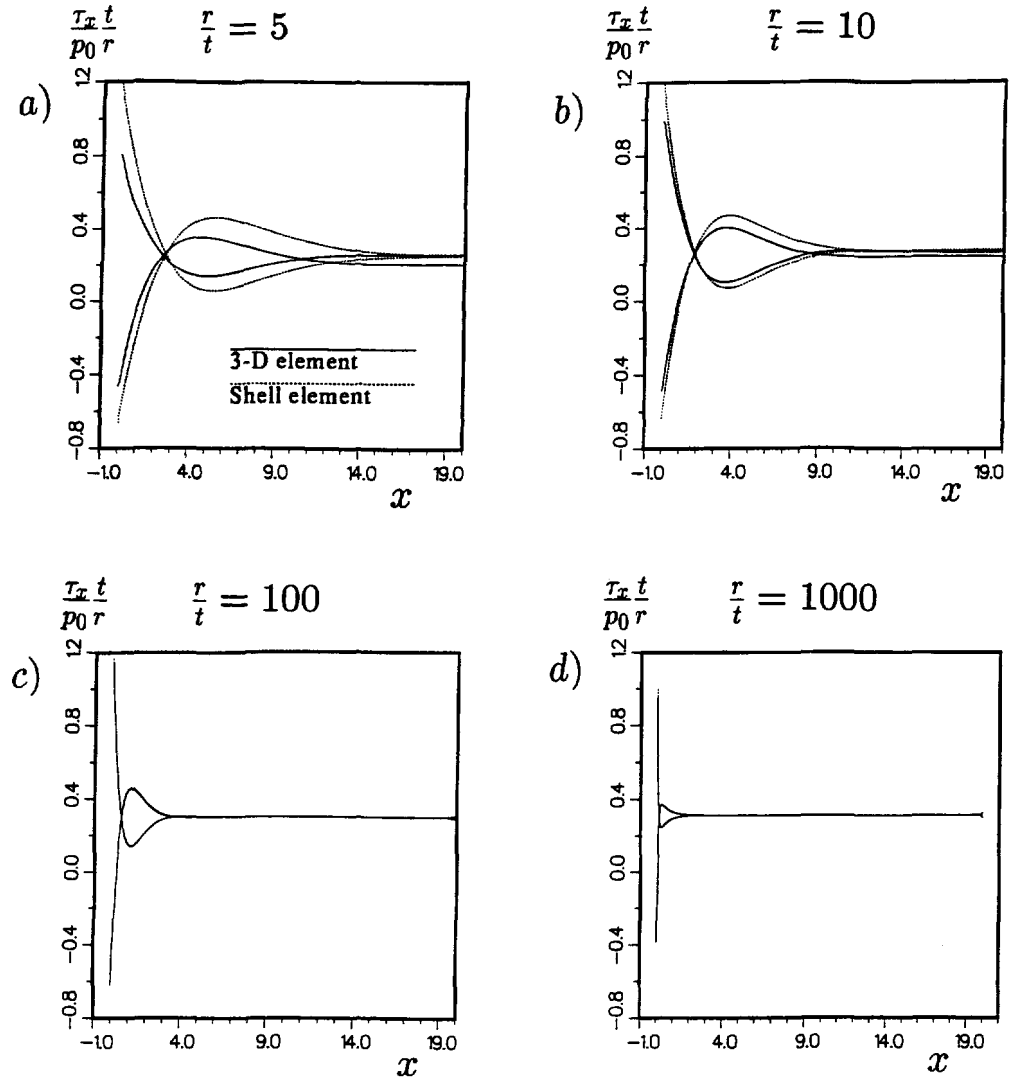

Fig. 4. Axial Kirchhoff stresses at Gauss points.

effect which is due to the too-coarse discretization. Notably, the curves of the three-dimensional element are much smoother, even for the 16×16 discretization. In the range $v > 180$ the three-dimensional element shows a slightly stiffer load–deformation behaviour than the shell element. The plastic boundaries for different deformation states are depicted in Fig. 7. A good agreement between the shell and the three-dimensional solution is obtained. Obviously, the three-dimensional element exhibits a wider plastic zone. This is due to the fact that for the three-dimensional formulation the stresses were projected on the nodes, whereas for the shell the calculation was carried out at the Gauss points.

5. CONCLUSION

The main aim of this paper was a comparison of modelling shells by three-dimensional brick elements and simple shell elements. It has been shown in the examples that the enhanced strain brick element yields accurate solutions of shell problems, even for very thin shells up to $r/t \approx 10^4$. For thinner shells, from the computational effort, an equivalent discretization with brick elements leads to an ill-conditioned system of equations, but even here no locking can be observed. Thus in total we can conclude that the three-dimensional brick element can be applied for thin shell problems. However, further investigations

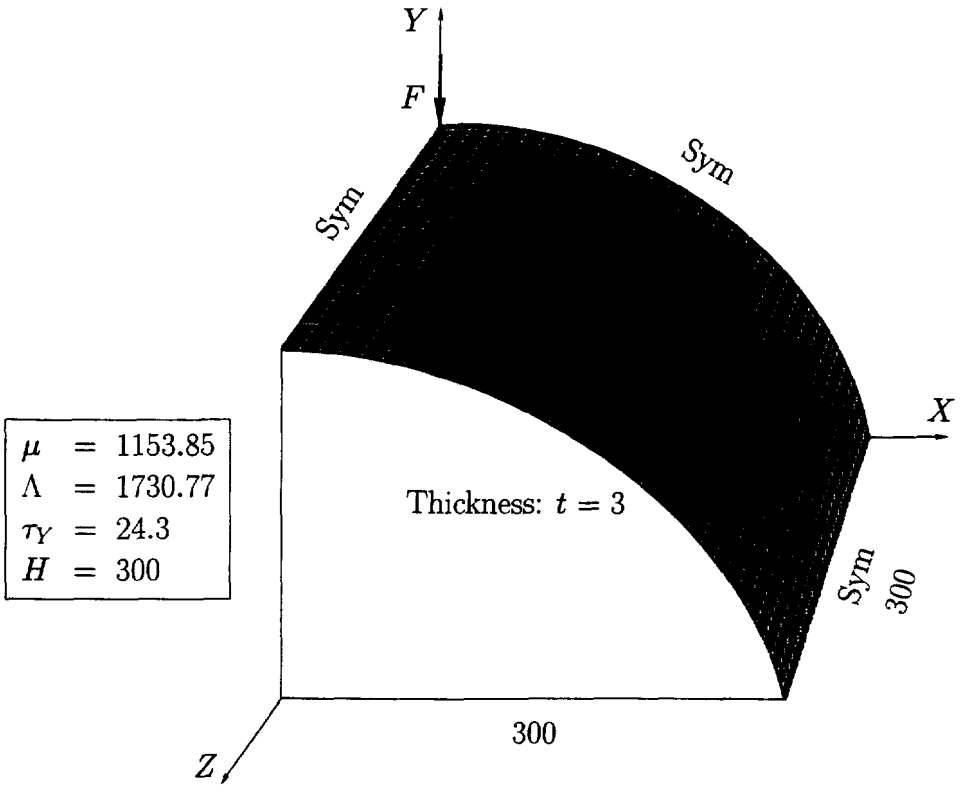

Fig. 5. Discretization of the pinched cylinder.

(a)

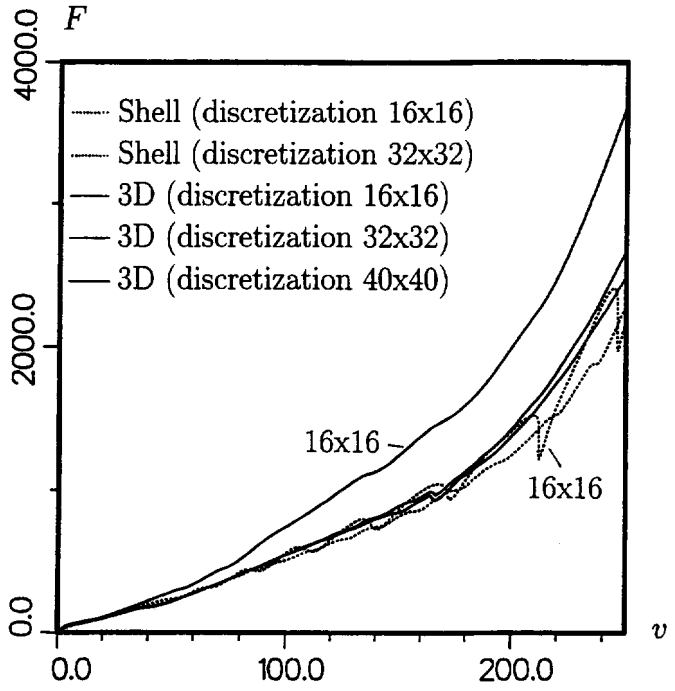

(b)

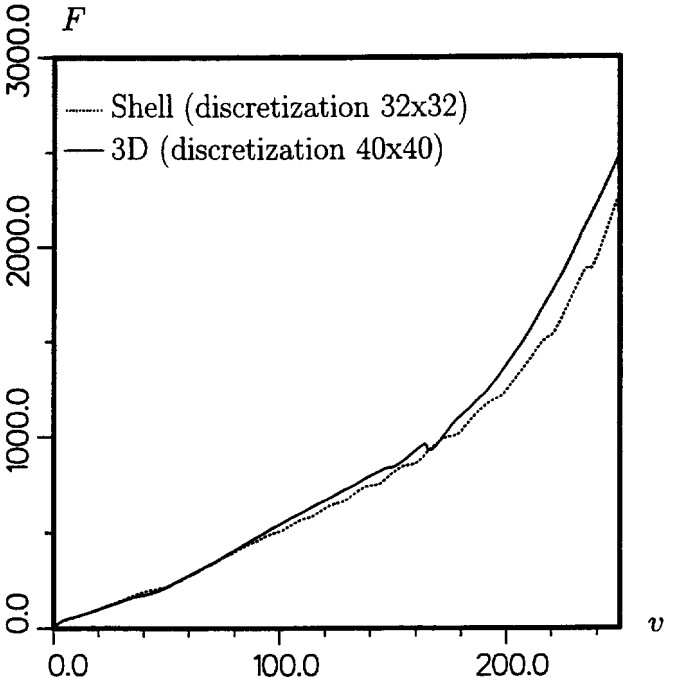

Fig. 6. Load–deformation curves.

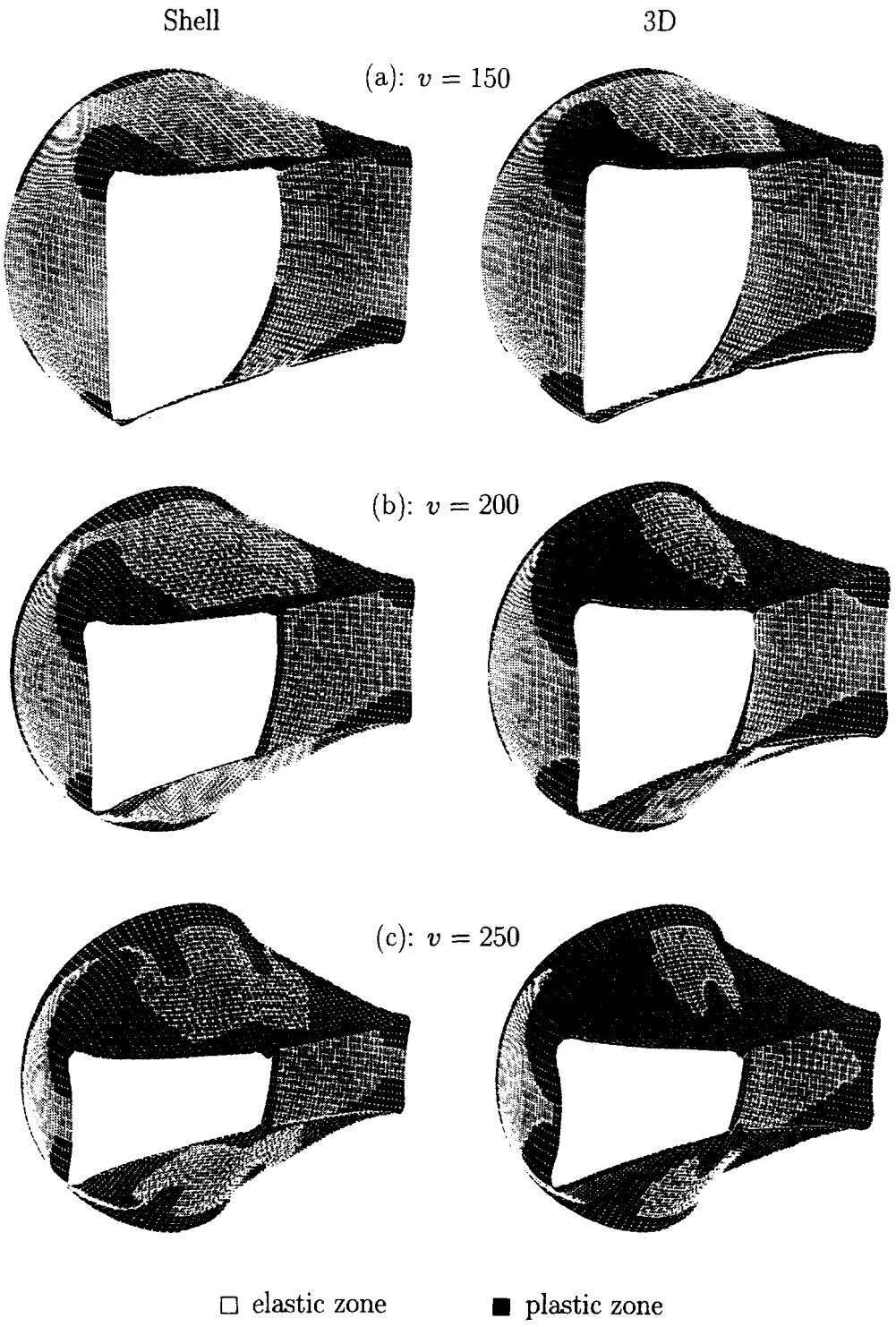

Fig. 7. Evolution of the plastic zone.

regarding the element behaviour in unstructured meshes have to be carried out, which is essential for adaptive techniques.

REFERENCES

Basar, Y. and Ding, Y. (1990). Theory and finite element formulation for shell structures undergoing finite rotations. In *Advances in the Theory of Shells and Plates* (Edited by G. T. Voyiadjis and D. Karamanlidis), pp. 3–26. Elsevier, Amsterdam.

Büchter, N., Ramm, E. and Roehl, D. (1994). Three-dimensional extension of non-linear shell formulation based on the enhanced assumed strain concept. *Int. J. Numer. Meth. Engng* **37,** 2551–2568.

Eberlein, R., Wriggers, P. and Taylor, R. L. (1993). A fully non-linear axisymmetrical quasi-Kirchhoff-type shell element for rubber-like materials. *Int. J. Numer. Meth. Engng* **36,** 4027–4043.

Hughes, T. J. R. and Liu, W. K. (1981). Nonlinear finite element analysis of shells: Part I. Three-dimensional shells. *Comput. Meth. Appl. Mech. Engng* **26,** 331–362.

Ibrahimbegović, A. (1994). Finite elastoplastic deformations of space-curved membranes. *Comput. Meth. Appl. Mech. Engng* **119,** 371–394.

Korelc, J. and Wriggers, P. (1995). An efficient three-dimensional enhanced strain element with Taylor expansion of the shape functions. *Comput. Mech.* submitted.

Morman, K. N. (1986). The generalized strain measure with application to nonhomogeneous deformations in rubber-like solids. *J. Appl. Mech.* **53,** 726–728.

Ogden, R. W. (1984). *Nonlinear Elastic Deformation.* Ellis Horwood, Chichester.

Parisch, H. (1991). An investigation of a finite rotation four-node shell element. *Int. Numer. Meth. Engng* **31,** 127–150.

Ramm, E. (1976). Geometrisch nichtlineare Elastostatik und finite Elemente. Report No. 76-2, Institut für Baustatik, Universität Stuttgart.

Reese, S. (1994). Theorie und Numerik des Stabilitätsverhaltens hyperelastischer Festkörper. Dissertation, Institut für Mechanik, Technische Hochschule Darmstadt.

Reese, S. and Wriggers, P. (1995). A finite-element method for stability problems in finite elasticity. *Int. J. Numer. Meth. Engng* **38,** 1171–1200.

Schoop, H. (1986). Oberflächenorientierte schalentheorien endlicher verschiebungen. *Ing. Archiv* **56,** 427–437.

Schweizerhof, K. and Ramm, E. (1984). Displacement dependent pressure loads in nonlinear finite-element analysis. *Comput. Struct.* **18,** 1099–1114.

Sewell, M. J. (1966). On configuration-dependent loading. *Arch. Rational Mech. Anal.* **23,** 327–351.

Simo, J. C. (1992). Algorithms for static and dynamic multiplicative plasticity that preserve the classical return mapping schemes of the Infinitesimal Theory. *Comput. Meth. Appl. Mech. Engng* **99,** 61–112.

Simo, J. C. and Armero, F. (1992). Geometrically nonlinear enhanced-strain mixed methods and the method of incompatible modes. *Int. J. Numer. Meth. Engng* **33,** 1413–1449.

Simo, J. C. and Kennedy, J. G. (1992). On a stress resultant geometrically exact shell model. Part V. Nonlinear plasticity: formulation and integration algorithms. *Comput. Meth. Appl. Mech. Engng* **96,** 133–171.

Simo, J. C. and Ortiz, M. (1985). A unified approach to finite deformation elastoplasticity based on the use of hyperelastic constitutive equations. *Comput. Meth. Appl. Mech. Engng* **46,** 201–215.

Simo, J. C. and Rifai, M. S. (1990). A class of mixed assumed strain methods and the method of incompatible modes. *Int. J. Numer. Meth. Engng* **29,** 1595–1638.

Simo, J. C. and Miehe, C. (1992). Coupled associative thermoplasticity at finite strains. Formulation, numerical analysis and implementation. *Comput. Meth. Appl. Mech. Engng* **98,** 41–104.

Simo, J. C. and Taylor, R. L. (1991). Quasi-incompressible finite elasticity in principal stretches. Continuum basis and numerical algorithms. *Comput. Meth. Appl. Mech. Engng* **85,** 273–310.

Simo, J. C., Fox, D. D. and Rifai, M. S. (1990). On a stress resultant geometrically exact shell model. Part III. Computational aspects of the nonlinear theory. *Comput. Meth. Appl. Mech. Engng* **79,** 21–70.

Simo, J. C., Taylor, R. L. and Wriggers, P. (1991). A note on finite-element implementation of pressure boundary loading. *Commun. Appl. Numer. Meth.* **7,** 513–525.

Simo, J. C., Armero, F. and Taylor, R. L. (1993). Improved versions of assumed enhanced-strain tri-linear elements for three-dimensional finite deformation problems. *Comput. Meth. Appl. Mech. Engng* **110,** 359–386.

Wagner, W. and Gruttmann, F. (1994). A simple finite rotation formulation for composite shell elements. *Engng Comput.* **11,** 145–176.

Wriggers, P. and Gruttmann, F. (1993). Thin shells with finite rotations formulated in Biot stresses theory and finite-element-formulation. *Int. J. Numer. Meth. Engng* **36,** 2049–2071.

Wriggers, P. and Hueck, U. (1995). A formulation of the QS6-element for large elastic deformations. *Int. J. Numer. Meth. Engng* **65,** 465–477.

Wriggers, P., Eberlein, R. and Gruttmann, F. (1995). An axisymmetrical quasi-Kirchhoff-type shell element for large plastic deformations. *Arch. Appl. Mech.* In press.

Zienkiewicz, O. C., Too, J. and Taylor, R. L. (1971). Reduced integration technique in general analysis of plates and shells. *Int. J. Numer. Meth. Engng* **3,** 275–290.